H. E. MERRITT
Section Head,
Hydraulic Systems Section,
Product Development Department,
The Cincinnati Milling Machine Company,
Cincinnati, Ohio

Theory of Self-Excited Machine-Tool Chatter

Contribution to Machine-Tool Chatter Research—1

Self-excited chatter, an instability of the cutting process in combination with the machine structure, is a basic performance limitation of a machine tool. A theory is developed which permits calculation of borderlines of stability for a structure having n-degrees of freedom and assuming no dynamics in the cutting process. Harmonic solutions of the system characteristic equation are found using a special chart, and the resulting data are used to plot a stability chart. However, an infinite number of such stability charts exists for a given machine because the structure dynamics vary with cutting-force orientation. This fact makes a simpler index of chatter performance desirable. A simple stability criterion is proposed which states that the directional cutting stiffness must be less than one half the minimum directional dynamic stiffness of the structure for each force orientation to assure chatter-free performance at all spindle speeds. Thus chatter-free performance can be fundamentally identified with adequate structural dynamic stiffness for all cutting-force orientations. Such a broad requirement for dynamic stiffness is difficult to meet in the design stage since structural characteristics are not easily predicted and controlled. Machine testing with continual improvements in the structure to increase dynamic stiffness is currently the best way to combat chatter.

Introduction

Chatter is a nuisance to metal cutting and can be demonstrated on any chip-producing machine tool. The effects of chatter are all adverse and affect surface finish, dimensional accuracy, tool life, and machine life.

Undulations in the surface finish are commonly referred to as chatter or chatter marks. A great many factors contribute to chatter marks. In the case of milling, the basic mechanics of the cutting process itself results in undulations (cutter marks) in the finish. Velocity variations in slide motion, perhaps caused by unbalance in the drive system, servo instability, or stick-slip friction, can result in periodic variations in the finish. However, forced and self-excited vibrations are the major sources of the finish problem referred to as chatter.

Forced vibrations can result from unbalance of rotating members and/or impacts by a multitooth cutter. The theory of forced vibrations is rather well developed compared to the self-excited type. In practice, chatter resulting from forced vibrations is traced by comparing the frequency of chatter to the frequency of possible forcing functions. Once the driving force causing the chatter is identified, the driving force and/or the dynamic compliance (inverse of dynamic stiffness) spectrum of the machine structure are reduced to permissible values.

The violent chatter often observed during cutting is caused by self-excited vibrations. The theory of self-excited chatter has taken on increased importance because of advancements in machining speed and the machining of thermal-resistant alloys. In recent years many theories [1, 2, 3][1] have been proposed to explain self-excited chatter, but no single theory covers all the effects observed.

A typical stability chart for a machine tool is shown in Fig. 1. An examination of this chart will aid in defining clearly the problem of computing self-excited chatter and indicate the achievement of published theories toward the solution of this problem. Referring to Fig. 1, three borderlines of stability can be identified which for classification purposes will be called *lobed*, *tangent*, and *asymptotic*. The lobed borderline of stability is the exact borderline and may be approximated with the asymptotic borderline or more closely with the tangent borderline. The

Contributed by the Production Engineering Division and presented at the Winter Annual Meeting, New York, N. Y., November 29–December 3, 1964, of The American Society of Mechanical Engineers. Manuscript received at ASME Headquarters, August 10, 1964. Paper No. 64—WA/Prod-13.

[1] Numbers in brackets designate References at end of paper.

Nomenclature

C = machining constant (usually on the order of 75 deg), deg

$c_1, c_2, c_3, \ldots$ = damping coefficients of modes of vibration of structure, lb sec/in.

F = resultant cutting force or vector force exciting the structure, lb

f = frequency, cps

f_0 = chatter frequency along lobed borderline of stability, cps

$g_1, g_2, g_3, \ldots$ = directional factors, dimensionless

G_m = normalized dynamic compliance of structure, dimensionless

k_c = static directional cutting stiffness (slope of curve of F versus u), lb/in.

k_d = minimum directional dynamic stiffness in dynamic stiffness spectrum of structure, lb/in.

k_m = directional static stiffness of structure (slope of curve of F versus y), lb/in.

$k_1, k_2, k_3, \ldots$ = spring constants of modes of vibration of structure, lb/in.

m = equivalent mass of structure, lb sec^2/in.

N = spindle speed, rps

n, an integer = number of degrees of freedom of structure, dimensionless; integer number of cycles cut on workpiece (during chatter) between tool tip and tool face, cycles

S_s = mean shear strength of metal being cut, psi

s = Laplace operator, sec^{-1}

T = delay time between tool tip and tool face ($T = 1/N$ for lathe, $T = 1/2N$ for drill, and $T =$

(Continued on next page)

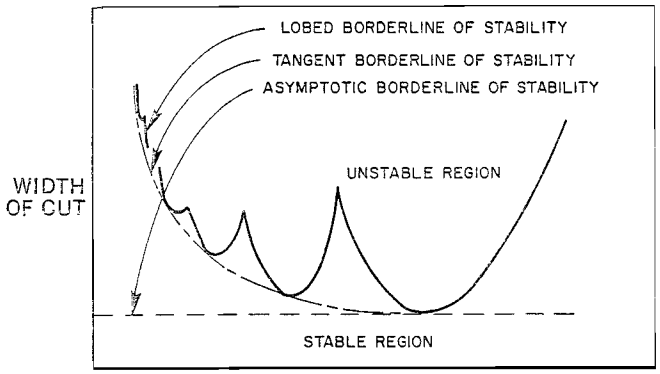

Fig. 1 Typical stability chart for a machine tool

asymptotic, tangent, and lobed borderlines of stability are progressively more difficult to compute but, fortunately, are progressively less important from a practical viewpoint. Each of these borderlines may be attributed to a particular physical phenomenon.

The asymptotic borderline of stability is the principal borderline since it defines the maximum width of cut which will result in stable cutting at *all* speeds. If spindle speed is chosen carefully, especially at lower speeds, then the tangent and lobed borderlines may indicate a larger stable width of cut. However, this method of speed selection is not practical since a different stability chart exists for each orientation of the resultant cutting force and for each possible position of the movable elements of a machine tool.

Several theories have been published which gave calculation procedures for some stability borderlines. Tlusty [4] has solved the important problem of computing the asymptotic borderline for a structure with n-degrees of freedom assuming negligible cutting dynamics. Tobias and Fishwick [5, 6, 7] have made an exact solution to the three borderlines of stability for a structure with one degree of freedom and have developed the concept of penetration rate to account for the region of stability at lower speeds; i.e., the area bounded by the asymptotic and tangent borderlines. However, the concept of penetration rate has not met with general acceptance since other explanations exist for this region [13]. If this region is not accounted for, then the tangent borderline becomes coincident with the asymptotic borderline.

Gurney and Tobias [8] and Peters [9] have published similar approaches to the problem of computing the asymptotic and lobed borderlines of stability for a structure with n-degrees of freedom and assuming negligible cutting-process dynamics. However, these techniques are computationally inconvenient to apply.

The purpose of this paper is to show that self-excited chatter can be represented by a feedback loop. Analysis of this loop using feedback control theory yields a straightforward method of calculating the asymptotic and lobed borderlines of stability for a machine-tool system with a structure having n-degrees of freedom and assuming negligible cutting-process dynamics.

Derivation of Chatter Loop

In order to derive the feedback loop representing chatter, the cutting process will be illustrated with a single-point tool performing orthogonal cutting on a lathe as shown in Fig. 2. The tool is mounted rigidly and the feed rate is adjusted to obtain an average or steady-state depth of cut, $u_0(t)$. In this steady-state condition, the structure maintains a certain deflection caused by the steady-state cutting force. Equations will be written about this point of equilibrium.

Uncut Chip-Thickness Equation

Referring to Fig. 2, the instantaneous depth of cut, $u(t)$, is decreased as the workpiece moves away from the cutting tool; i.e., as $y(t)$ increases. Further, if the workpiece moves away from the tool, a lump is left on the workpiece. This lump increases the uncut chip thickness one revolution of the work or T sec later. Hence the instantaneous uncut chip thickness can be written

$$u(t) = u_0(t) - y(t) + \mu y(t - T) \qquad (1$$

where

$$T = \frac{1}{N}$$

and μ is the overlap factor. The overlap factor accounts for the overlapping of successive cuts; i.e., it defines the portion of the previous cut which overlaps the present cut. In a turning operation such as threading, the previously machined surface does not

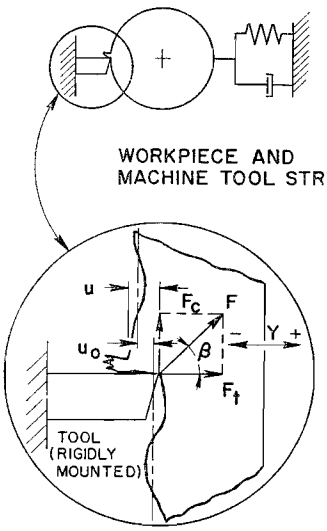

Fig. 2 Cutter in a turning operation

Nomenclature

$1/zN$ for milling machine), sec
t = time, sec
u = instantaneous uncut chip thickness, in.
u_0 = average or steady-state uncut chip thickness, in.
w_1 = width of cut (measured along cutting edge of tool), in.
y = relative displacement between tool and workpiece normal to machined surface, in.
z = total number of cutting edges on cutter
α = top rake angle of tool, deg
$\alpha_1, \alpha_2, \alpha_3, \ldots$ = angle of modes of vibration of structure relative to a line normal to machined surface, deg
β = angle between resultant cutting force and a line normal to machined surface, deg
$\delta_1, \delta_2, \delta_3, \ldots$ = damping ratios of modes of vibration of structure, dimensionless
$\delta_a, \delta_b, \delta_c, \ldots$ = damping ratios of numerator quadratic factors of dynamic compliance of structure, dimensionless
μ = overlap factor, dimensionless
ν = phase factor—a fractional portion of a cycle cut on workpiece (during chatter) between tool tip and tool face, cycles
τ = friction angle, deg
$\omega = 2\pi f$ = angular frequency, rad/sec
$\omega_1, \omega_2, \omega_3, \ldots$ = undamped natural frequencies of modes of vibration of structure, rad/sec
$\omega_a, \omega_b, \omega_c, \ldots$ = undamped natural frequencies of numerator quadratic factors of dynamic compliance of structure, rad/sec

affect the present uncut chip thickness and, therefore, $\mu = 0$. However, for most machining operations, such as orthogonal cutting, $\mu = 1$.

The overlap factor also may be used to account for the geometrical effects of rounding at the tool cutting edge and of tool clearance angle. Both of these effects tend to smear the machined surface and thereby reduce the amplitude of periodic variations in the machined surface. It is difficult to make a precise definition for μ; however, it is certainly bounded between zero and unity; i.e., $0 \leq \mu \leq 1$. An overlap factor of unity is the most critical value from the viewpoint of chatter.

Laplace transforming equation (1) yields

$$u(s) = u_0(s) - y(s) + \mu e^{-Ts}y(s) \tag{2}$$

Cutting-Process Equation

The resultant cutting force, $F(t)$, is related to the instantaneous uncut chip thickness, $u(t)$, by the dynamics of the cutting process. The differential equations describing the dynamic behavior of the cutting process have not been written from the physics of metal cutting. Although much work has been done on cutting process dynamics [10–13], a definitive experimental result has not been published. However, the steady-state behavior of the cutting process has been analyzed by Merchant [14]. If the dynamics are neglected, then Merchant's equations can be combined to give

$$F(t) = k_c u(t) \tag{3}$$

where k_c is the static directional cutting stiffness, or simply cutting stiffness, and is given by

$$k_c = \frac{2w_1 S_s}{\sin C - \sin(\tau - \alpha)} \tag{4}$$

The quantities S_s, C, and τ in equation (4) are determined by the workpiece material, and α is obtained from the tool geometry. Therefore, the cutting stiffness is directly proportional to the width of cut for a given workpiece material and tool geometry.

Laplace transforming equation (3) gives

$$F(s) = k_c u(s) \tag{5}$$

The direct proportionality between resultant cutting force and uncut chip thickness is the simplest approximation that can be made to the cutting process.

Structure Equation

The vector cutting force acts to displace the workpiece and the structure of the machine. Therefore the dynamic compliance characteristic of the structure is of interest from the viewpoint of chatter. Machine-tool structures are continuous systems and, therefore, are described by partial differential equations. These are formidable equations with complex boundary conditions and constraints. In most cases the dynamic compliance may be approximated adequately using a lumped-parameter analysis. If the structure could be represented by a lumped-parameter model with one degree of freedom, as shown in Fig. 3(*a*), then the force equation is

$$F(t)\cos(\alpha_1 - \beta) = m\frac{d^2}{dt^2}\left[\frac{y(t)}{\cos\alpha_1}\right] + c_1\frac{d}{dt}\left[\frac{y(t)}{\cos\alpha_1}\right] + k_1\left[\frac{y(t)}{\cos\alpha_1}\right]$$

which may be Laplace transformed to give the following dynamic compliance:

$$\frac{y(s)}{F(s)} = \frac{1}{k_m\left[\frac{s^2}{\omega_1^2} + \frac{2\delta_1 s}{\omega_1} + 1\right]} \tag{6}$$

where

$$g_1 = \cos(\alpha_1 - \beta)\cos\alpha_1,\ \omega_1^2 = k_1/m,\ \delta_1 = c_1/2(k_1 m)^{1/2}$$

and $1/k_m = g_1/k_1$

The dynamic compliance of a lumped-parameter model representing a structure with two degrees of freedom, Fig. 3(*b*), can be shown to be

$$\frac{y(s)}{F(s)} = \frac{g_1}{k_1\left[\frac{s^2}{\omega_1^2} + \frac{2\delta_1}{\omega_1}s + 1\right]} + \frac{g_2}{k_2\left[\frac{s^2}{\omega_2^2} + \frac{2\delta_2}{\omega_2}s + 1\right]} \tag{7}$$

where $g_1 = \cos(\alpha_1 - \beta)\cos\alpha_1$, $g_2 = \cos(\alpha_2 - \beta)\cos\alpha_2$, $\omega_1^2 = k_1 m$, $\omega_2^2 = k_2 m$, $\delta_1 = c_1/2(k_1 m)^{1/2}$, and $\delta_2 = c_2/2(k_2 m)^{1/2}$. The right side of equation (7) may be written with a common denominator to obtain the conventional time-constant form for a transfer function. Therefore

$$\frac{y(s)}{F(s)} = \frac{\left(\frac{s^2}{\omega_a^2} + \frac{2\delta_a}{\omega_a}s + 1\right)}{k_m\left(\frac{s^2}{\omega_1^2} + \frac{2\delta_1}{\omega_1}s + 1\right)\left(\frac{s^2}{\omega_2^2} + \frac{2\delta_2}{\omega_2}s + 1\right)} \tag{8}$$

where

$$\frac{1}{k_m} = \frac{g_1}{k_1} + \frac{g_2}{k_2},\ \omega_a^2 = \frac{g_1\omega_2^2 + g_2\omega_1^2}{g_1 + g_2},$$

and

$$\delta_a = \frac{g_1\omega_2\delta_2 + g_2\omega_1\delta_1}{(g_1 + g_2)\omega_a}$$

In general, the response of a structure with n-degrees of freedom can be written, if the system is linear, as [15]

$$\frac{y(s)}{F(s)} = \frac{\left(\frac{s^2}{\omega_a^2} + \frac{2\delta_a}{\omega_a}s + 1\right)\left(\frac{s^2}{\omega_b^2} + \frac{2\delta_b}{\omega_b}s + 1\right)\cdots}{k_m\left(\frac{s^2}{\omega_1^2} + \frac{2\delta_1}{\omega_1}s + 1\right)\left(\frac{s^2}{\omega_2^2} + \frac{2\delta_2}{\omega_2}s + 1\right)\left(\frac{s^2}{\omega_3^2} + \frac{2\delta_3}{\omega_3}s + 1\right)\cdots} \tag{9}$$

where k_m is the directional static stiffness; ω_1, ω_2, ... are the undamped natural frequencies of the modes of vibration; ω_a, ω_b, ... are the undamped natural frequencies of numerator quadratic factors. The number of denominator quadratic factors corresponds to the number of degrees of freedom, and the number of numerator quadratic factors is always at least one less than that of the denominator. Excitation at forcing frequencies corresponding to denominator and numerator undamped natural frequencies results in points of minimal and maximal dynamic

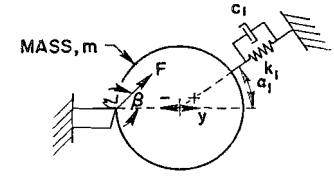

a. ONE DEGREE OF FREEDOM

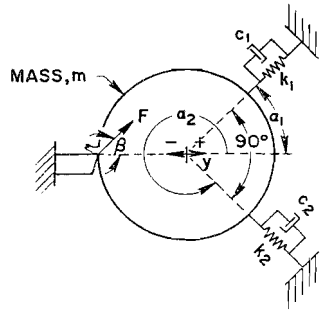

b. TWO DEGREES OF FREEDOM

Fig. 3 Structures with one and two degrees of freedom

stiffness, respectively, in the frequency spectrum. It is convenient symbolically to write the dynamic compliance, equation (9), in the form

$$\frac{y(s)}{F(s)} = \frac{1}{k_m} G_m(s) \tag{10}$$

where $G_m(s)$ represents the normalized dynamic compliance.

The force exciting the structure during chatter, the resultant cutting force, is a space vector. Therefore, a different dynamic compliance exists for each possible orientation of the cutting-force vector and, further, for each possible position of the movable elements of a machine. Thus it is not theoretically possible to describe a structure with a unique dynamic compliance, and whether it is practically possible remains to be resolved.

Since it is not presently possible to compute all the quantities required to define a mode of vibration, the dynamic compliance of a structure must be obtained experimentally for each possible machining operation. The relative displacement, $y(t)$, is measured normal to the instantaneous cut surface because variations (chatter) in this direction affects the uncut chip thickness. A dynamic compliance for a structure having three degrees of freedom is shown in Fig. 4. The value of minimum dynamic stiffness (maximum dynamic compliance) will be of significance and is noted in Fig. 4.

Block Diagram of Chatter Loop

Equation (2), (5), and (10) are the three basic equations required to define the system. The cutting process is directly coupled to the structure, and the uncut chip-thickness equation provides the feedback tie necessary for the possibility of chatter. The interdependence of the three basic equations can best be seen in the block diagram, Fig. 5, of these equations. Two feedback paths can be distinguished: A negative feedback of position (primary path) and a positive feedback of delayed position (regenerative path). The primary feedback path is always present; the regenerative path may or may not be present because it depends on the value of the overlap factor. If $\mu = 0$, then chatter occurring will be designated *primary chatter;* otherwise, chatter will be termed *regenerative chatter.*

Referring to Fig. 5, the depth of cut initially set, $u_0(s)$, is the reference or input quantity; the actual depth of cut, $u(s)$, is the controlled or output quantity. This situation is entirely analogous to a servo loop where a controlled quantity is directly related to a reference. The transfer function relating $u_0(s)$ and $u(s)$ can be obtained by solving the three basic equations simultaneously or directly from the block diagram. Therefore

$$\frac{u(s)}{u_0(s)} = \frac{1}{1 + (1 - \mu e^{-Ts}) \dfrac{k_c}{k_m} G_m(s)} \tag{11}$$

If either the dynamic compliance of the structure or the cutting stiffness is zero, then the actual depth of cut is equal to the set depth of cut. Since the chatter loop may be treated as a servo loop, all the performance indexes of a servo loop (such as absolute and relative stability, bandwidth, accuracy, and so on) can be found for the chatter loop. However, only one aspect of performance, that of stability, is of interest in the chatter problem.

Stability of Chatter Loop

A linear system is stable, by definition, if its impulse response decays with time. This definition of stability can be translated into the following mathematical requirement: A linear lumped-parameter system is stable if, and only if, all roots of its characteristic equation have negative real parts. If any or all of the roots have positive real parts, then the system is unstable. If any of the roots have zero real parts, the rest having negative real parts, then this condition represents the borderline of stability and solutions of the characteristic equation are harmonic.

Referring to equation (11) the characteristic equation of the chatter loop can be identified as

$$1 + (1 - \mu e^{-Ts}) \frac{k_c}{k_m} G_m(s) = 0 \tag{12}$$

and stability requires that the roots of this equation be confined to the left half of the s-plane; i.e., none may be permitted on the imaginary axis or in the right half of the s-plane. Roots on the imaginary axis are of the form $s = j\omega$ and correspond to harmonic solutions. These solutions must be found to define the borderline of stability.

Substituting $s = j\omega$ into equation (12) and rearranging

$$\frac{k_c}{k_m} G_m(j\omega) = \frac{-1}{1 - \mu e^{-j\omega T}} \tag{13}$$

The left side of this equation is the product of the harmonic response functions of the cutting process and the structure; that is

$$\frac{y(j\omega)}{u(j\omega)} = \frac{F(j\omega)}{u(j\omega)} \frac{y(j\omega)}{F(j\omega)} = \frac{k_c}{k_m} G_m(j\omega) \tag{14}$$

Therefore y/u is obtained by multiplying the dynamic compliance of the structure by k_c. The right side of equation (13) will be denoted

$$G_{cp} = \frac{-1}{1 - \mu e^{-j\omega T}} \tag{15}$$

whose plot can be considered a locus of critical points. Substituting equations (14) and (15) into equation (13) yields

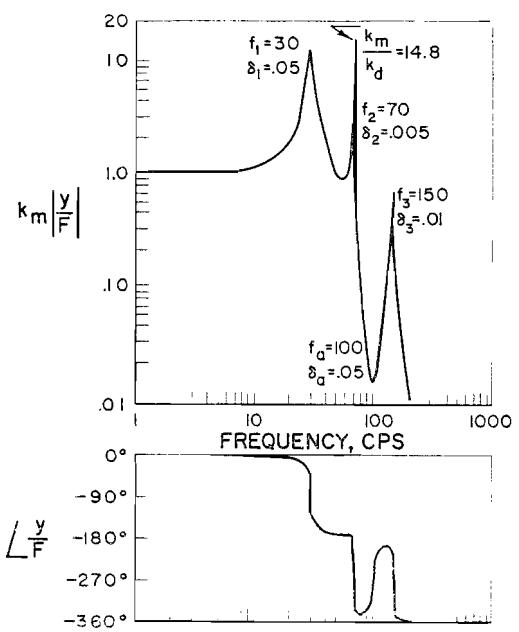

Fig. 4 Dynamic compliance of a structure with three degrees of freedom

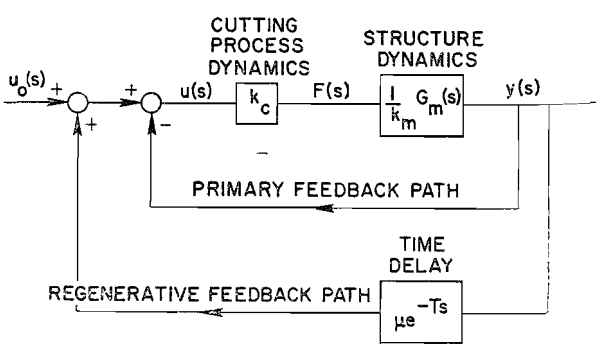

Fig. 5 Block diagram of chatter loop

$$\frac{y(j\omega)}{u(j\omega)} = G_{cp} \tag{16}$$

Intersections of the plot of y/u with points on the critical locus give harmonic solutions of the characteristic equation which define the borderline of stability. Absence of harmonic solutions, i.e., absence of intersections, does not necessarily, in general, imply system stability; this must be established from other information. However, in this case, intersections occur only for sufficiently large values of cutting stiffness. This correlates with experimental observations of chatter occurring for sufficiently large widths of cut. Therefore, if the plot of y/u does not intersect any point defined by G_{cp}, then the system is *absolutely stable;* i.e., stable at all speeds.

The critical locus, given by G_{cp}, is a function of μ and a periodic function of ωT. The quantity ωT is the phase angle in radians of the regenerative wave on the machined surface at the face of the tool relative to the wave actually being cut. It is convenient to express this phase angle as an integral number of cycles, n, plus a fractional portion of a cycle, ν; that is

$$\omega T = 2\pi(n + \nu) = 2\pi f T \tag{17}$$

where ν is defined as the phase factor and has a range $0 \leq \nu \leq 1$. Since n is an integer, $e^{-j2\pi n} = 1$ and, therefore, $e^{-j2\pi(\nu+n)} = e^{-j2\pi\nu}$. Thus, the equation describing the critical locus can be written

$$G_{cp} = \frac{-1}{1 - \mu e^{-j2\pi\nu}} \tag{18}$$

and may be uniquely plotted as a function of μ and ν. It is shown in the Appendix that contours of constant μ and constant ν are circles on a polar plot, and these contours are plotted in Fig. 6.[2] Note that for $\mu = 1$, the critical locus is a line parallel to the imaginary axis through the point $-0.5 + j0$; if the system is to be stable at all speeds, then the plot of y/u cannot enter the region to the left of this line. Therefore, $\mu = 1$ imposes serious constraints on stability. As μ decreases toward zero, the plot of y/u cannot enter the regions within the circles if the system is to be stable at all speeds. For $\mu = 0$, the critical region reduces to a geometric point, $-1 + j0$, which is the conventional Nyquist critical point.

A stability chart may be plotted from information given by the points of intersection. At an intersection point, a value for f is obtained from the plot of y/u and a value for ν is obtained from the appropriate (μ-contour) locus of critical points. Equation (17) can be written

$$\frac{1}{T} = \frac{f}{\nu + n} \tag{19}$$

Critical speeds ($N = 1/T$ for a lathe) are computed using equation (19) with $n = 0, 1, 2, 3, \ldots$

Examples of Computed Stability Charts

Let us consider two examples to illustrate the stability theory developed in the preceding section. The theory consists of making a polar plot of the function y/u, equation (14), on specially prepared paper having contours of constant μ and constant ν. As the width of cut is gradually increased, then k_c is increased and the plot of y/u expands and intersects with the appropriate μ-contour. If k_c is of such a value that no intersections occur, then the system is absolutely stable; if intersections occur then the system is unstable at speeds given by equation (19).

The theory leads to use of the critical loci plotted in polar form, Fig. 6; however, from a computational viewpoint, polar plotting is not the best choice. The linear-amplitude ratio scale on polar paper does not permit convenient plotting of large ranges and, further, the graph of y/u must be computed and plotted for each value of k_c. Use of a gain-phase plot of the critical loci, as shown in Fig. 7, avoids these inconveniences. A gain-phase plot of y/u is made on transparent paper which is then superimposed on the plot of critical loci. As k_c is increased, the plot of y/u is shifted vertically until intersections occur.

For example, consider a structure which can be approximated by a model with one degree of freedom. The dynamic compliance is given by equation (6), and let us assume that $f_1 = 30$ cps and $\delta_1 = 0.05$. Therefore,

$$\frac{y(s)}{u(s)} = \frac{k_c/k_m}{\left(\frac{s}{2\pi\ 30}\right)^2 + \frac{2(0.05)}{2\pi\ 30}s + 1}$$

Substituting in $s = j\omega = j\ 2\pi\ f$, the corresponding harmonic-response function is obtained.

$$\frac{y}{u} = \frac{k_c/k_m}{1 - \left(\frac{f}{30}\right)^2 + j\ 2(0.05)\frac{f}{30}} \tag{20}$$

A gain-phase plot of this function is superimposed on the plot of critical loci and slid upward until the first intersection occurs as

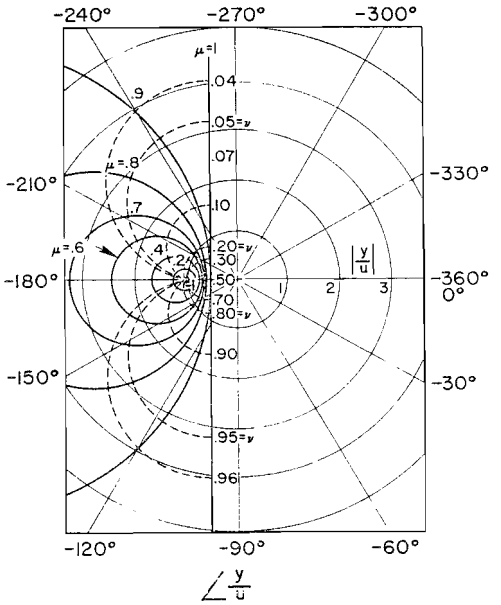

Fig. 6 Polar plot of critical loci

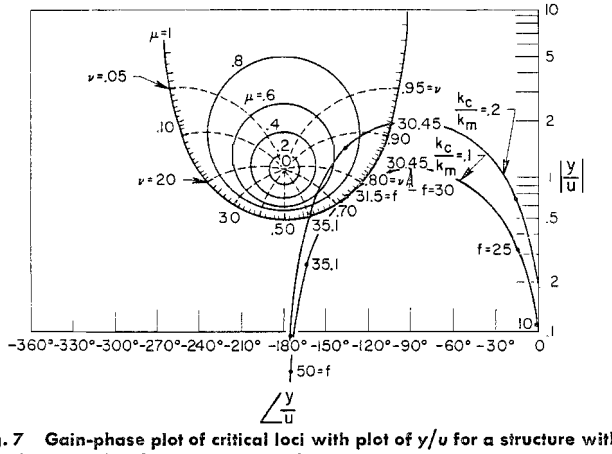

Fig. 7 Gain-phase plot of critical loci with plot of y/u for a structure with one degree of freedom superimposed

[2] Although these contours have the same equation as that of M and α-contours of a Nichol's chart in feedback control theory, their interpretation is entirely different. M-contours of a Nichol's chart define a measure of relative stability; intersection with an M-contour does not indicate instability. However, μ-contours are loci of critical points, and intersection with a μ-contour indicates instability.

Table 1 Tabulation of intersection points and critical speeds

k_c/k_m	f, cps	ν	Critical speeds, rps $n = 0$	$n = 1$	$n = 2$	$n = 3$	$n = 4$
0.105	31.5	0.758	42.4	18.1	11.5	8.42	6.65
0.12	30.8	0.843	36.5	16.7	10.85	8.0	6.36
	32.62	0.67	48.7	19.5	12.2	8.89	6.98
0.15	30.56	0.884	34.5	16.2	10.6	7.86	6.25
	33.65	0.63	53.4	20.65	12.8	9.26	7.28
0.20	30.45	0.916	33.2	15.9	10.43	7.77	6.20
	35.1	0.6	58.8	22.	13.5	9.75	7.63
0.50	30.24	0.968	31.2	15.35			
	42.35	0.545	77.7	27.4			
1.0	30	0.99	30.1				
	52	0.526	98.8				

shown in Fig. 7 (assuming $\mu = 1$). This first intersection gives values of $k_c/k_m = 0.105$, $f = 31.5$ cps, and $\nu = 0.758$ cycles; the critical speeds for a lathe are then $N = 31.5/(0.758 + n) = 42.4, 18.1, 11.5, 8.42, 6.65, 5.48$ rps, and so on. As k_c/k_m is increased further, say, to $k_c/k_m = 0.20$ as shown in Fig. 7, there are two points of intersection with values of $f = 30.45$ cps, $\nu = 0.916$ cycles and $f = 35.1$ cps, $\nu = 0.6$ cycles. Critical speeds for these two points are $N = 30.45/(0.916 + n) = 33.2, 15.9, 10.43, 7.77$, and so on, and $N = 35.1/(0.6 + n) = 58.5, 22, 13.5, 9.75$, and so on, respectively. Therefore as k_c/k_m is progressively increased, two points of intersection occur and the data from these points with the computed critical speeds are used to construct the tabulation shown in Table 1. Note from the table for $n = 0$ that when $k_c/k_m = 0.105$ the critical speed is 42.4 and when $k_c/k_m = 0.12$ the critical speeds are 36.5 and 48.7 which bracket the speed of 42.4 rps. As k_c/k_m increases, each successive critical speed range brackets the former speed range for a given value of n and defines a lobe of the stability chart. The stability chart, shown in Fig. 8 for this example, is a superposition of the lobes which occur for $n = 0, 1, 2, 3$, and so on. As n increases the overlapping of the lobes become more pronounced so that large values of n need not be considered. The chatter frequency, f_0, along the lobed borderline of stability, also shown in Fig. 8, gives a somewhat saw-toothed characteristic typical of chatter [5]. Note also in Fig. 8 that the asymptotic and tangent borderlines of stability are coincident and given by $k_c/k_m = 0.105$. It can be shown easily that the asymptotic borderline of stability is given by

$$\frac{k_c}{k_m} = 2\delta_1 + 2\delta_1^2 \qquad (21)$$

when the structure has one degree of freedom. Referring to Fig. 8 and assuming a width of cut such that $k_c/k_m = 0.15$, note that as speed is increased there are bands of chatter-free performance; this type of behavior is typical of chatter. Machine operators often vary speed, among other things, in an effort to eliminate chatter.

It is important to note from the first example that a single point of intersection of the two loci (locus of y/u and critical locus) gave rise, as k_c/k_m was increased, to a complete lobed borderline of stability. As a second example, consider a structure with three degrees of freedom having the dynamic compliance shown in Fig. 4. A gain-phase plot of y/u is made and superimposed on the critical loci (let $\mu = 1$) as shown in Fig. 9. As k_c/k_m is increased, note that there are two basic single-point intersections ($k_c/k_m = 0.055$, $f = 69.6$, $\nu = 0.28$; $k_c/k_m = 0.09$, $f = 31.6$, $\nu = 0.75$) each of which will give a complete lobed borderline of

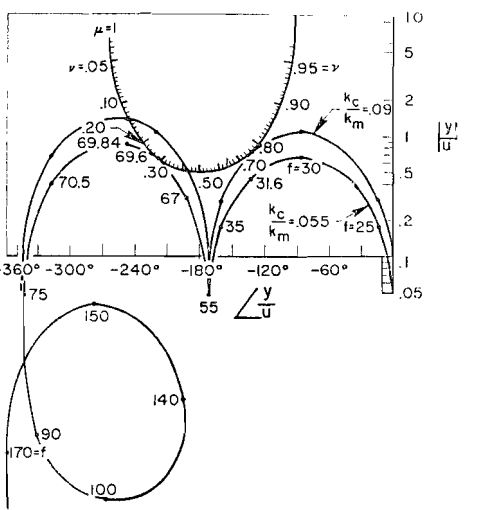

Fig. 9 Gain-phase plot of critical loci with plot of y/u for a structure with three degrees of freedom superimposed

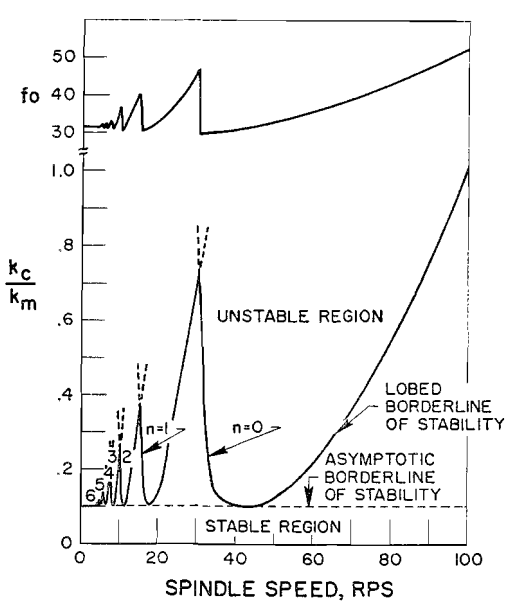

Fig. 8 Stability chart for a system with a structure having one degree of freedom

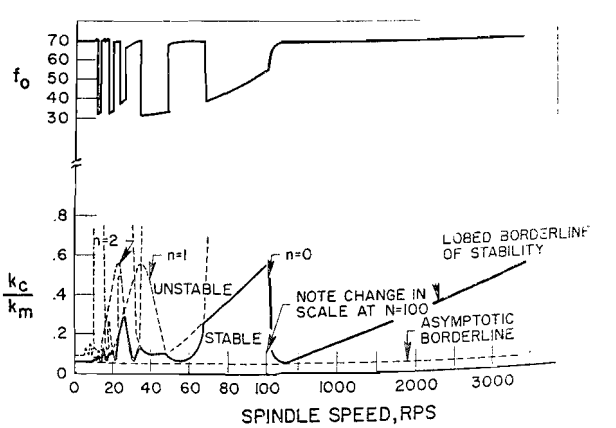

Fig. 10 Stability chart for a system with a structure having three degrees of freedom

stability. A tabulation of data similar to Table 1 can be made and the two lobed borderlines are plotted in Fig. 10. A third basic intersection will occur (at $k_c/k_m = 1.5, f = 148.3$, and $\nu = 0.23$) but the resulting borderline is not significant since it is enclosed by the other borderlines. These two borderlines, because of modes at 30 cps and 70 cps, overlap to form the solid curve in Fig. 10 which is the exact or lobed borderline of stability for this case. The chatter frequency along the borderline of stability is also plotted in Fig. 10. Note the jumps in frequency from near 30 cps to near 70 cps. The asymptotic borderline occurs at $k_c/k_m = 0.055$ since this value gives the largest chatter-free width of cut at all speeds.

It is apparent from this example that the exact borderline of stability can be very complex when several modal frequencies are significant since a superposition of many individual borderlines is involved. Extreme care would have to be used in measuring such a stability chart in order to detect chatter bands. However, chatter frequency can serve as a clue in complex cases since abrupt changes occur when more than one mode is involved in the chatter. Also the quantity n, the number of integer cycles on the workpiece between tool tip and tool face, can be a guide in measurements. If n is large, which occurs at lower spindle speeds, there is much overlapping of lobes and chatter-free bands are less distinct. If n is small then such bands should be detectable. Quite possibly, especially at low n-values, an experimental value for ν could be obtained and interpreted.

Physical interpretation of the lobes can be made. The lobe for $n = 0$ corresponds to a fraction, ν, of a period cut on the workpiece. There is one complete period and a fraction for $n = 1$, and two complete periods and a fraction for $n = 2$, and so on. Thus by simply counting the number of chatter marks an indication of chatter bands is obtained. When there are many such marks, the lobes overlap extensively and chatter-free bands may not be detectable unless spindle speed is controlled precisely. If all experimental evidence is evaluated carefully, then measured and computed stability charts should agree.

A Simplified Stability Criterion

Although the theory is somewhat involved, the construction of a stability chart for a given structure compliance is a relatively routine task. However, the practicality of stability charts as an index of chatter performance is another matter. Many factors complicate the usefulness of such stability charts.

1 There is not a unique stability chart for a given machine because the dynamic compliance is not unique. This is the most serious difficulty; all other difficulties are minor in comparison.

2 The dynamic compliance of a structure, both amplitude and phase, is not easily measured. However, this difficulty could be overcome with adequate test equipment.

3 It is difficult, if not impossible, to obtain a precise value for the overlap factor.

4 The lobed and tangent borderlines are too involved to be of practical value.

With these comments it is obvious that simplifications must be made. Let us choose $\mu = 1$, since this value is the most pessimistic for chatter, and examine the requirements for the asymptotic borderline of stability. Referring to Fig. 6, it is apparent that no intersections will occur if the minimum (i.e. the most negative) real part of y/u, which will be denoted

$$\frac{k_c}{k_m} \operatorname{Re}[G_m(j\omega)]_{\min}$$

is greater than $-1/2$. That is, the system is stable at all speeds if

$$\frac{k_c}{k_m} \operatorname{Re}[G_m(j\omega)]_{\min} > -\frac{1}{2} \tag{22}$$

Equating both sides yields the cutting stiffness for the asymptotic borderline of stability. Therefore

$$k_c = -\frac{k_m}{2\operatorname{Re}[G_m(j\omega)]_{\min}} \tag{23}$$

This result was first obtained by Tlusty [4]. It is too complex for use as a chatter criterion since measurement of the real part of the structural compliance is required.

A simpler chatter performance index can be obtained by referring to Fig. 6 and observing that absolute stability is assured if the plot of y/u is confined to a circle with radius of $1/2$; that is, absolute stability will result if

$$\left|\frac{y}{u}\right| = \frac{k_c}{k_m} |G_m(j\omega)| < \frac{1}{2} \tag{24}$$

Now the maximum value of the structure dynamic compliance is $1/k_d$. Therefore

$$\frac{k_c}{k_d} < \frac{1}{2} \tag{25}$$

and the simple borderline of stability is given by

$$k_c = \frac{k_d}{2} \tag{26}$$

This stability criterion requires that the minimum dynamic stiffness be measured for all possible cutting-force orientations. This is still a difficult experimental job, but phase measurement is not required. Let us apply this criterion to the two examples discussed. If the structure has one degree of freedom it can be shown that $k_d = 2\delta_1(1 - \delta_1^2)^{1/2}k_m$ so that the simple stability borderline is given by $k_c = \delta_1(1 - \delta_1^2)^{1/2}k_m$. For the first example $\delta_1 = 0.05$ and the simple criterion gives $k_c = 0.0499\ k_m$ which roughly compares with the asymptotic borderline at $k_c = 0.105\ k_m$. For the second example, $k_d = k_m/14.8$ and the simple criterion gives $k_c = 0.0338\ k_m$ which compares fairly well with the asymptotic borderline at $k_c = 0.055\ k_m$. The simple stability criterion is always conservative and gives a better approximation in complex cases than for simple cases.

Conclusions

A chatter theory has been developed which permits computation of asymptotic and lobed borderlines of stability for a machined-tool system having a structure with n-degrees of freedom and described by a measured dynamic compliance. Dynamics of the cutting process are neglected. Harmonic solutions of the system characteristic equation define the borderline of stability and are found by superimposing a plot of y/u, which is the product of cutting stiffness and structural dynamic compliance, on a special chart of critical loci. Points of intersection define harmonic solutions and give all the data required to plot a stability chart. Although the theory is illustrated by a single-point tool in a turning proces it should be extendable to other metal-cutting processes.

Stability charts are complicated and a multiplicity of such charts exists for a particular machine tool. A simple stability criterion which relates directly to the minimum dynamic stiffness of the structure is proposed as an index of chatter performance.

Fundamentally, chatter is caused by a lack of adequate dynamic stiffness (for all cutting-force orientations) in the machine structure. This difficulty can be traced to the lack of damping inherent in structures. If damping ratios on the order of $\delta = 0.5$ were characteristic of structures, chatter would still be possible but it would be a relatively minor problem. It is the dynamic stiffness which results in the principal region of stability enclosed by the asymptotic borderline. Lobes on the stability chart, which result in alternate bands of chatter and chatter-free performance, are caused by the regenerative effect of the machined surface. The region of stability at lower speeds enclosed by the tangent borderline is not yet fully resolved but may be deduced to be a result of geometry and/or dynamics of the

cutting process. These comments give a physical explanation for the three basic features (borderlines of stability) of a typical stability chart.

A theory of chatter offers few clues to the design of chatter-free machines. However, it does indicate the scope of the problem. The most significant result is the emphasis on structures with higher dynamic stiffness (lower dynamic compliance), but this fact has been known (except for the confusion of weight for rigidity and static for dynamic stiffness) for a long time. The chatter loop is complicated and about the only portion of the loop under the designer's control is the structure, which is very complex. The prevention of chatter will remain a difficult task for the machine-tool designer until techniques are developed to improve structure dynamic stiffness.

Acknowledgments

This work was performed as part of a general effort toward understanding of the chatter problem supported by United States Air Force Contract No. AF 33(657)-9143, ASD Project No. 7-771, under the direction of Mr. Floyd L. Whitney. The author would like to express his appreciation to Mr. J. T. Gavin, Dr. J. R. Lemon, and Dr. R. Hahn for their valuable assistance in formulating the problem and to Dr. P. Schultheiss and Dr. R. Sridhar for stimulating discussions concerning the application of Nyquist's criterion to this problem.

References

1 C. Andrew and S. A. Tobias, "A Critical Comparison of Two Current Theories of Machine Tool Chatter," *International Journal of Machine Tool Design Research*, vol. 1, 1961, pp. 325–335.

2 R. N. Arnold, "Mechanism of Tool Vibration in Cutting of Steel," *Proceedings of The Institution of Mechanical Engineers*, London, vol. 154, 1946, pp. 261–276.

3 R. S. Hahn, "On the Theory of Regenerative Chatter in Precision-Grinding Operations," TRANS. ASME, vol. 76, 1954, pp. 593–597.

4 J. Tlusty and M. Polacek, "Beispiele der Behandlung der selbsterregten Schwingung der Werkzeugmaschinen," 3. *FoKoMa*, Vogel-Verlag Wuerzburg, October, 1957.

5 S. A. Tobias, "The Vibrations of Vertical Milling Machines Under Test and Working Conditions," *Proceedings of The Institution of Mechanical Engineers*, London, vol. 173, 1959, pp. 474–506.

6 S. A. Tobias and W. Fishwick, "The Chatter of Lathe Tools Under Orthogonal Cutting Conditions," TRANS. ASME, vol. 80, 1958, pp. 1079–1088.

7 S. A. Tobias and W. Fishwick, "The Vibrations of Radial-Drilling Machines Under Test and Working Conditions," *Proceedings of The Institution of Mechanical Engineers*, London, vol. 170, 1956, pp. 232–264.

8 J. P. Gurney and S. A. Tobias, "A Graphical Method for the Determination of the Dynamic Stability of Machine Tools," *International Journal of Machine Tool Design Research*, vol. 1, 1961, pp. 148–156.

9 J. Peters, "Un Critère de Stabilité Dynamique pour Machines-Outels," Center de Recherches Scientifiques et Technique de L'industrie des Fabrications Metalliques, Study no. 13, August, 1962.

10 J. A. Smith and S. A. Tobias, "The Dynamic Cutting of Metals," *International Journal of Machine Tool Design Research*, vol. 1, 1961, pp. 283–292.

11 Shumsheruddin and S. Tobias, "Dynamic Metal Cutting," Third International Machine Tool Design and Research Conference, September 26, 1962.

12 S. Doi and S. Kato, "Chatter Vibration of Lathe Tools," TRANS. ASME, vol. 78, 1956.

13 R. L. Kegg, "Cutting Dynamics in Machine Tool Chatter," in this issue, pp. 464–470.

14 M. E. Merchant, "Basic Mechanics of the Metal-Cutting Process," *Journal of Applied Mechanics*, vol. 11, TRANS. ASME, vol. 66, 1944, p. A-168.

15 G. W. Long and J. R. Lemon, "Structural Dynamics in Machine Tool Chatter," in this issue, 455–463.

APPENDIX

It will now be shown that contours of constant μ and contours of constant ν are circles when plotted on a polar (or rectangular) diagram. Equation (18) can be rearranged so that

$$\frac{1}{\mu} e^{j2\pi\nu} = \frac{G_{cp}}{1 + G_{cp}} \tag{27}$$

Since G_{cp} is a complex quantity, it can be written in the form $G_{cp} = x + jy$. Substitution into equation (27) gives

$$\frac{1}{\mu} e^{j2\pi\nu} = \frac{x + jy}{1 + x + jy} \tag{28}$$

Converting both sides of equation (28) to polar form and simplifying

$$\frac{1}{\mu} \angle 360\,\nu = \frac{(x^2 + y^2)^{1/2}}{[(1 + x)^2 + y^2]^{1/2}} \angle \tan^{-1}\frac{y}{x} - \tan^{-1}\frac{y}{1 + x} \tag{29}$$

Equation (29) may be written as the following two equations:

$$\frac{1}{\mu} = \frac{(x^2 + y^2)^{1/2}}{[(1 + x)^2 + y^2]^{1/2}} \tag{30}$$

$$360\,\nu = \tan^{-1}\frac{y}{x} - \tan^{-1}\frac{y}{1 + x} \tag{31}$$

Equation (30) may be manipulated algebraically to give

$$\left(x + \frac{1}{1 - \mu^2}\right)^2 + y^2 = \left(\frac{\mu}{1 - \mu^2}\right)^2 \tag{32}$$

Therefore, contours of constant μ on a polar (or rectangular) plot are circles with center at

$$\left(-\frac{1}{1 - \mu^2} + j0\right)$$

and radius of $\mu/(1 - \mu^2)$.

Taking the tangent of both sides of equation (31) yields

$$\tan(360\nu) = \tan\left[\tan^{-1}\frac{y}{x} - \tan^{-1}\frac{y}{1 + x}\right] \tag{33}$$

The trigonometric identity

$$\tan(\alpha - \beta) = \frac{\tan\alpha - \tan\beta}{1 + \tan\alpha\tan\beta} \tag{34}$$

may be used to evaluate the right side of equation (33).

Therefore,

$$\tan(360\,\nu) = \frac{\dfrac{y}{x} - \dfrac{y}{1 + x}}{1 + \dfrac{y}{x}\left(\dfrac{y}{1 + x}\right)} \tag{35}$$

which may be manipulated algebraically to obtain

$$(x + \tfrac{1}{2})^2 + \left[y - \frac{1}{2\tan(360\,\nu)}\right]^2 = \left\{\frac{1}{2}\left(1 + \frac{1}{[\tan(360\,\nu)]^2}\right)^{1/2}\right\}^2 \tag{36}$$

Therefore, contours of constant ν on a polar (or rectangular) plot are circles with center at

$$\left[-\frac{1}{2} + j\frac{1}{2\tan(360\,\nu)}\right]$$

and radius of

$$\frac{1}{2}\left\{1 + \frac{1}{[\tan(360\,\nu)]^2}\right\}^{1/2}$$

It is further apparent that these circles always go through the points $(-1 + j0)$ and $(0 + j0)$.